Delineating antibody escape from Omicron variants

Henning Gruell[1], Kanika Vanshylla[1], Michael Korenkov[1], Pinkus Tober-Lau[2], Matthias Zehner[1], Friederike Münn[2], Hanna Janicki[1], Max Augustin[3], Philipp Schommers[1,3], Leif Erik Sander[2], Florian Kurth[2,4], Christoph Kreer[1], Florian Klein[1,5,6,*]

1 Laboratory of Experimental Immunology, Institute of Virology, Faculty of Medicine and University Hospital Cologne, University of Cologne, Cologne, Germany
2 Department of Infectious Diseases and Respiratory Medicine, Charité-Universitätsmedizin Berlin, Freie Universität Berlin and Humboldt-Universität zu Berlin, Berlin, Germany
3 Department I of Internal Medicine, Faculty of Medicine and University Hospital Cologne, University of Cologne, Cologne, Germany
4 Department of Tropical Medicine, Bernhard Nocht Institute for Tropical Medicine and Department of Medicine I, University Medical Center Hamburg-Eppendorf, Hamburg, Germany
5 German Center for Infection Research (DZIF), Partner site Bonn-Cologne, Cologne, Germany
6 Center for Molecular Medicine Cologne (CMMC), University of Cologne, Cologne, Germany

* Correspondence should be addressed to florian.klein@uk-koeln.de.

Summary

SARS-CoV-2-neutralizing antibodies play a critical role for protection and treatment of COVID-19. Viral antibody evasion therefore threatens essential prophylactic and therapeutic measures. The high number of mutations in the Omicron BA.1 sublineage results in markedly reduced neutralization susceptibility. Consistently, Omicron is associated with lower vaccine effectiveness and a high re-infection rate. Notably, newly emerging Omicron sublineages (BA.1.1, BA.2) have rapidly become dominant. Here, we determine polyclonal serum activity against BA.1, BA.1.1 and BA.2 in 50 convalescent or vaccinated individuals as well as delineate antibody sensitivities on a monoclonal level using 163 antibodies. Our study reveals a significant but comparable reduction of serum activity against Omicron sublineages which markedly increases after booster immunization. However, notable differences in sensitivity to individual antibodies demonstrate distinct escape patterns of BA.1 and BA.2 that also affect antibodies in clinical use. The results have strong implications for vaccination strategies and antibody use in prophylaxis and therapy.

Introduction

Following its emergence two years into the COVID-19 pandemic, the Omicron variant of SARS-CoV-2 has resulted in a global surge of infections (Viana et al., 2022). Although Omicron is associated with reduced pathogenicity, its high transmissibility poses a considerable threat to individuals at risk and the public health system (Madhi et al., 2022; Meng et al., 2022; Shuai et al., 2022). Moreover, high rates of breakthrough infections in immunized individuals are clinical manifestations of its immune evasive properties (Altarawneh et al., 2022; Andrews et al., 2022; Madhi et al., 2022; Tseng et al., 2022). Omicron's marked resistance to neutralizing antibodies induced by vaccination or previous infection is mediated by a high number of mutations in the spike protein (Cao et al., 2022; Carreno et al., 2022; Cele et al., 2022; Garcia-Beltran et al., 2022; Gruell et al., 2022; Hoffmann et al., 2022; Liu et al., 2022; Planas et al., 2022; Schmidt et al., 2022; VanBlargan et al., 2022). These include mutations that have rendered several therapeutic monoclonal antibodies ineffective (Gruell et al., 2022; Liu et al., 2022; VanBlargan et al., 2022). Prolonged vaccine dosing intervals and booster immunizations based on the ancestral Wu01 strain of SARS-CoV-2 elicit Omicron-neutralizing serum activity (Cheng et al., 2022; Garcia-Beltran et al., 2022; Gruell et al., 2022; Perez-Then et al., 2022; Schmidt et al., 2022; Wratil et al., 2022; Zhao et al., 2022). However, serum titers against Omicron remain lower compared to those against other variants and Omicron breakthrough infections are frequently observed (Kuhlmann et al., 2022). Most experimental evidence on the resistance of the Omicron variant to antibody-mediated neutralization is limited to analyses of the initial BA.1 strain. However, as additional sublineages emerge (Qassim et al., 2022; Yamasoba et al., 2022), determining their escape properties is of critical importance to effectively guide preventive and therapeutic measures. Therefore, we

61 determined in detail antibody-mediated neutralization of the prevalent Omicron
62 sublineages (BA.1, BA.1.1, and BA.2), both on a polyclonal and monoclonal level.
63
64 **Results**
65
66 **Rapid spread of Omicron sublineages**
67 Compared to the Wu01 strain of SARS-CoV-2, the spike protein of BA.1 differs in 39 amino
68 acid residues (**Figure 1A**). While recently emerged sublineages of Omicron share several
69 BA.1 mutations, they differ at various amino acid positions and therefore can alter critical
70 epitopes (**Figures 1A** and **1B**). For example, the spike protein of sublineage BA.1.1
71 contains an additional R346K substitution in the receptor-binding domain (RBD) that was
72 previously observed in the Mu variant of SARS-CoV-2 and has been associated with escape
73 from neutralizing antibodies (**Figure 1A**) (Greaney et al., 2021). Moreover, BA.2 shares
74 only 21 (68%) of its 31 spike protein amino acid changes with BA.1 (**Figure 1A**).
75 Therefore, BA.2 differs considerably from BA.1 and BA.1.1 in both the N-terminal domain
76 (NTD) and the RBD, regions targeted by the most potent SARS-CoV-2-neutralizing
77 antibodies (**Figure 1A**). While BA.1 and BA.1.1 dominated the initial surge of Omicron
78 infections, they have already been outcompeted by BA.2 in numerous countries (**Figure**
79 **1C**). Therefore, the BA.2 omicron sublineage is likely to dominate the SARS-CoV-2
80 pandemic in the near future.
81
82 **Comparable reduction of serum neutralizing activity against Omicron sublineages**
83 We analyzed serum neutralizing activity using lentivirus-based pseudovirus assays
84 against the ancestral Wu01 strain as well as BA.1, BA.1.1, and BA.2 Omicron sublineages
85 (Crawford et al., 2020; Vanshylla et al., 2021). To this end, we collected samples from two

longitudinal cohorts of i.) SARS-CoV-2-convalescent individuals (*n*=20) and ii.) vaccinated health care workers (*n*=30) (**Table S1**) (Hillus et al., 2021; Vanshylla et al., 2021). In both cohorts, individuals received an mRNA booster immunization (BNT162b2) after a median of 14 and 9 months following infection or two doses of BNT162b2, respectively.

Convalescent individuals had a median age of 51 years (interquartile range [IQR] 35-58) and were diagnosed with mild or asymptomatic SARS-CoV-2 infection. Early post-infection samples (V1) were collected at a median of 48 days (IQR 35-58) after disease onset and neutralizing activity was assessed by determining the 50% inhibitory serum dilutions (ID_{50}s) (**Figure 2A**). Neutralization of the Wu01 strain was detected in all samples (100%) obtained early after infection, with individual ID_{50} values ranging from 16 to 3,200 (geometric mean ID_{50} [GeoMeanID_{50}] of 322) (**Figure 2B**). In contrast, serum activity against Omicron sublineages was strongly reduced and only detectable in 15%, 0%, and 50% for BA.1., BA1.1, and BA.2 respectively (**Figure 2B**). However, following booster immunization at a median of 33 days (IQR 27-54) in convalescent individuals, Omicron-neutralizing activity was elicited in all individuals (**Figures 2B**, **2C**, **S1A** and **S1B**), reaching GeoMeanID_{50}s of 1,688, 1,578, and 2,388 against BA.1, BA.1.1, and BA.2, respectively (**Figure 2B**).

In addition, we determined Omicron sublineage-neutralizing activity induced only by vaccination (**Figure 2D**). At a median of 28 days (IQR 27-32) after completion of the initial two-dose course of BNT162b2 (V1), Wu01-neutralizing serum activity was detected in all 30 individuals with a GeoMeanID_{50} of 585 (**Figure 2E**). Although Omicron sublineage-neutralization was detectable in 43-73% of vaccinated individuals, GeoMeanID_{50}s against BA.1, BA.1.1., and BA.2 were low at 11, 8, and 15, respectively (**Figure 2E**). Follow-up samples obtained at a median of 29 days (IQR 26-35) after booster immunization showed 8-fold higher activity against Wu01 (GeoMeanID_{50} of 4,817) and

strongly increased Omicron activity in all individuals with GeoMeanID_{50}s of 648 against BA.1, 557 against BA.1.1, and 592 against BA.2 (**Figures 2E**, **S1C**, and **S1D**). We conclude that booster immunizations are critical to elicit neutralizing serum activity against all prevalent Omicron sublineages in vaccinated as well as convalescent individuals. Notably, despite the differences in the spike proteins, Omicron sublineages were similarly affected on the level of serum neutralization.

Dissecting viral escape of Omicron sublineages

To decode Omicron escape from neutralizing antibodies, we produced and tested 158 monoclonal antibodies isolated from SARS-CoV-2-convalescent individuals against all Omicron sublineages. These included 67 randomly selected antibodies from the CoV-AbDab (Raybould et al., 2021), 79 antibodies isolated in our previous work (Kreer et al., 2020; Vanshylla et al., 2022), as well as 12 clinically evaluated antibodies. In total, this antibody panel originated from at least 43 different individuals out of 19 independent studies (**Figure 3A**, **Table S2**). The selection covered a broad spectrum of diverse SARS-CoV-2 neutralizing antibodies encompassing 92 V_H/V_L combinations. Most of these antibodies targeted the RBD (96.8 %) and included previously described public clonotypes such as the V_H3-53/3-66 subgroup (**Figure 3A**).

While all antibodies neutralized the Wu01 strain, only 18%, 17%, and 22% remained active against BA.1, BA.1.1, and BA.2, respectively (**Figure 3B**). Moreover, neutralization against Omicron sublineages was overall lower with GeoMeanIC_{50}s of 0.431 (BA.1), 0.506 (BA.1.1), and 0.178 (BA.2) compared to Wu-01-neutralizing antibodies (GeoMeanIC_{50} of 0.030 µg/mL; **Figure 3C**). However, our analysis identified a small number of antibodies with high potency against all Omicron sublineages, including antibodies isolated from individuals with outstanding serum activity (Vanshylla et al.,

2022). For example, antibodies R207-2F11 and R568-1G9 both neutralized BA.1, BA.1.1, and BA.2 with IC_{50}s <0.01 µg/ml (**Table S2**). Notably, antibodies maintaining Omicron-neutralizing activity carried a modest but significantly higher (5.2 vs. 6.9) number of V_H amino acid mutations (p=0.002), suggesting that a higher sequence diversification might be favorable for Omicron neutralization (**Figure S2**). Importantly, while antibody neutralization strongly correlated between BA.1 and BA.1.1 (r_s=0.858), a more divergent neutralization profile was observed when comparing BA.1 and BA.2 (r_s=0.763; **Figures 3D** and **3E**). Based on the analysis of the sublineage neutralization profiles, two prevalent classes of Omicron-neutralizing antibodies became apparent: i.) antibodies with comparable activity against BA.1 and BA.2 lineages (72.5% of antibodies), and ii.) antibodies with higher potency against BA.2 compared to BA.1 (25%) (**Figures 3E**, **3F**, and **3G**). While only a single (2.5%) out of the 40 Omicron-neutralizing antibodies showed >10-fold higher activity against BA.1 than BA.2, 10 out of 40 antibodies showed a 1.1 to 3.9 log_{10}-fold higher potency against BA.2 (**Figure 3G**). This indicates that based on the antibody panel tested, immune escape of BA.2 was less pronounced when compared to BA.1 and BA.1.1.

Finally, antibody responses against SARS-CoV-2 have previously been demonstrated to be highly convergent across individuals by the identification of several public clonotypes, which are conserved in terms of sequence characteristics and mechanisms of neutralization (Barnes et al., 2020; Nielsen et al., 2020; Robbiani et al., 2020; Yuan et al., 2020). Among the analyzed antibody panel, we identified 18 sequences from 11 individuals that could be assigned to a prominent V_H3-53/3-66|V_K1-9 clonotype (**Figure 3H**) (Cao et al., 2020; Vanshylla et al., 2022; Zhang et al., 2021). Interestingly, although these antibodies are highly conserved on a sequence level, they substantially differed in their Omicron neutralizing capacity (**Figure 3H**). For example, antibodies

R207-1C4 and R568-2G5 showed similar neutralizing activity against Wu01 and harbor eight amino acid mutations in their V_H gene segment (without CDRH3) of which five are at the same position and three are identical. However, R207-1C4 was not capable of neutralizing any Omicron variant, while R568-2G5 retained neutralizing activity against all variants. Notably, another member of this clonotype, C140, which has the identical CDRH3 motif as R568-2G5, did not neutralize any Omicron variant. These results indicate that minimal differences in antibody sequence characteristics can tip the scale between Omicron neutralization and resistance.

We conclude that the majority of Wu01-neutralizing antibodies lose activity against Omicron sublineages. While most BA.1-neutralizing antibodies were reactive against BA.1.1 and BA.2, the subset of antibodies with Omicron-neutralizing potency restricted towards BA.2 indicates differences in sublineage antigenicity. Moreover, the higher rate of BA.2- compared to BA.1-neutralizing monoclonal antibodies in our panel suggests that the BA.2 spike protein incorporates fewer features associated with resistance.

Impact of Omicron sublineages on clinical monoclonal antibodies

SARS-CoV-2-neutralizing monoclonal antibodies can reduce morbidity and mortality in infected individuals. Moreover, they are critical for passive immunization to protect individuals that do not mount an adequate immune response upon vaccination (Cohen et al., 2021; Corti et al., 2021; Dougan et al., 2021; Group, 2022; Gupta et al., 2021; O'Brien et al., 2021; Weinreich et al., 2021). To determine how spike protein mutations of Omicron sublineages affect antibodies in clinical use, we analyzed 9 monoclonal antibodies that received authorization for clinical use (**Figure 4A**) and 9 that are advanced in clinical development (**Figure S3**). All tested antibodies targeted the RBD of the SARS-CoV-2 spike

protein and were tested in parallel against Wu01 and the Omicron sublineages (**Figure 4B**).

Most antibodies showed highly potent neutralizing activity against Wu01 with IC_{50}s below 0.005 μg/ml (**Figure 4B**). Less potent and incomplete Wu01-neutralizing activity was observed for sotrovimab, which is consistent with previous reports showing reduced activity against pseudoviruses lacking the dominant D614G spike mutation (**Figure 4A**) (Liu et al., 2021; Weissman et al., 2021). In contrast to the high Wu01 activity, only 5 (28%) out of the 18 tested antibodies neutralized BA.1 with IC_{50}s <10 μg/ml. Moreover, in 2 out of these 5 antibodies, neutralizing activity was decreased by >2 log_{10} against BA.1 relative to Wu01 (**Figure 4B**). While the antibody neutralization profile against the BA.1.1 lineage was generally similar to that of BA.1, a few differences were detected. For example, DZIF-10c neutralized BA.1 with an IC_{50} of 0.046 μg/ml but completely lost activity against BA.1.1 (**Figure 4B**). Although the number of antibodies in clinical use with neutralizing activity against BA.2 remained small (5 out 18, 28%), the neutralization profile of BA.2 differed from that of BA.1 and BA.1.1 (**Figure 4B**). For example, antibody COV2-2130 (cilgavimab) neutralized BA.2 with high potency (IC_{50} of 0.008 μg/ml) that was similar to its activity against Wu01 and >800-fold higher than against BA.1 and BA.1.1 (**Figures 4A** and **4B**). In addition, while antibody imdevimab showed no appreciable activity against BA.1 and BA.1.1, neutralization of BA.2 was detectable at low levels (**Figures 4A** and **4B**). Out of all clinical antibodies tested, the recently authorized LY-CoV1404 (bebtelovimab) showed the highest levels of neutralizing activity against all Omicron sublineages (**Figures 4A** and **4B**).

We conclude that the prevalent Omicron sublineages are resistant to most monoclonal antibodies in clinical use and/or under investigation. Omicron sensitivity to these antibodies can, however, strongly differ on the sublineage level. Selection of

monoclonal antibodies for treatment or prevention of Omicron infection should therefore take sublineage identification and/or epidemiology into account.

Discussion

Neutralizing antibody-mediated immunity is a critical component of prophylactic and therapeutic measures against SARS-CoV-2 infection (Corti et al., 2021; Feng et al., 2021; Khoury et al., 2021). The COVID-19 pandemic has been characterized by ongoing viral evolution and periodic emergence of dominant variants in the context of increasing levels of population immunity that can drive selection of antibody resistance (Harvey et al., 2021). Soon after its appearance and explosive spread, considerable immune evasion of the highly mutated BA.1 sublineage of Omicron was confirmed both experimentally and clinically (Altarawneh et al., 2022; Andrews et al., 2022; Cao et al., 2022; Carreno et al., 2022; Cele et al., 2022; Garcia-Beltran et al., 2022; Gruell et al., 2022; Hoffmann et al., 2022; Liu et al., 2022; Madhi et al., 2022; Planas et al., 2022; Schmidt et al., 2022; Tseng et al., 2022; VanBlargan et al., 2022). However, novel Omicron sublineages with differing spike proteins have since become increasingly prevalent, suggesting higher immune escape and/or higher transmissibility (Lyngse et al., 2022; Qassim et al., 2022; Yamasoba et al., 2022). Establishing the impact of the new Omicron sublineages on polyclonal and monoclonal immunity is therefore critical to guide antibody-mediated strategies for prevention and treatment.

Our results demonstrate that Wu01-based mRNA vaccine boosters are effective in eliciting activity against the Omicron sublineages and result in comparable neutralizing titers against BA.1, BA.1.1, and BA.2. Although neutralizing activity against Omicron was considerably lower than against the ancestral strain, booster immunizations will therefore continue to be a critical component of vaccination strategies. In addition, our

236 analyses of a large antibody panel revealed similarities and differences in the sensitivity
237 of Omicron sublineages to antibodies isolated from SARS-CoV-2-convalescent individuals.
238 While the resistance profiles of BA.1 and BA.1.1 were largely overlapping, a substantial
239 fraction of antibodies with poor or no BA.1/BA.1.1-neutralizing activity showed high
240 activity against BA.2. Therapeutic monoclonal antibodies authorized for prevention or
241 treatment of SARS-CoV-2 infection were differentially affected, with some showing
242 increased and some showing reduced activity against BA.2 compared to BA.1, confirming
243 similar observations (Iketani et al., 2022). As the majority of tested antibodies failed to
244 neutralize any of the Omicron sublineages, highly potent antibodies identified by our
245 analysis may provide novel options for treatment and prevention in the Omicron era.
246 Our observations of higher pre-boost activity against BA.2, comparable
247 neutralization titers after booster immunization, as well the higher fraction of BA.2- than
248 BA.1-neutralizing monoclonal antibodies isolated from convalescent individuals suggest
249 that BA.2 overall does not have higher levels of antibody escape compared to BA.1.
250 Outcompetition of BA.1 by BA.2 therefore appears to driven rather by higher
251 transmissibility and/or other virological characteristics than by immune evasion.
252 However, as the rapid emergence of the highly resistant Omicron variant illustrated the
253 challenges posed by viral evolution, continuous genomic surveillance and assessments of
254 viral sensitivity will be critical for informing antibody-based prophylactic and therapeutic
255 measures.
256

257 **Acknowledgments**

258 We are grateful to all study participants for their dedication to our research. We thank F.
259 Dewald, L. Gieselmann, B. Kurt, C. Lehmann, P. Mayer, N. Riet, S. Salomon, M. Schlotz, R.
260 Schröder, R. Stumpf and H. Wüstenberg, as well as the members of the EICOV/COVIM

Study Group (Y. Ahlgrimm, L. Bardtke, K. Behn, N. Bethke, H. Bias, D. Briesemeister, C. Conrad, V. M. Corman, C. Dang-Heine, S. Dieckmann, C. Eroglu, D. Frey, J.-A. Gabelich, J. Gerdes, U. Gläser, A. Hetey, L. Hasler, E. T. Helbig, D. Hillus, W. Hirst, A. Horn, C. Hülso, S. Jentzsch, C. von Kalle, L. Kegel, A. Krannich, W. Koch, P. Kopankiewicz, P. Kroneberg, H. Le, L. J. Lippert, C. Lüttke, P. de Macedo Gomes, B. Maeß, C. Matthaiou, J. Michel, A. Nitsche, A.-M. Ollech, C. Peiser, A. Pioch, C. Pley, K. Pohl, C. Rubisch, L. Ruby, A. Sanchez Rezza, I. Schellenberger, V. Schenkel, J. Schlesinger, S. Schmidt, G. Schwanitz, T. Schwarz, J. Seybold, A. Solarek, A. Stege, S. Steinbrecher, P. Stubbemann, C. Thibeault, and D. Treue) for sample acquisition and processing; L. Buchholz and M. Wunsch for help with antibody production and preparation; and J.J. Malin for providing clinical antibody stocks. We thank all laboratories obtaining and submitting SARS-CoV-2 sequencing information to GISAID for facilitating rapid analyses of global variant distributions. This work was supported by grants from COVIM: NaFoUniMedCovid19 (FKZ: 01KX2021) (to L.E.S. and F. Klein), the Federal Institute for Drugs and Medical Devices (V-2021.3 / 1503_68403 / 2021–2022) (to L.E.S. and F. Kurth), the German Center for Infection Research (DZIF) (to F. Klein), and the Deutsche Forschungsgemeinschaft (DFG) CRC1310 (to C.K. and F. Klein).

Author contributions

Conceptualization, H.G., K.V., C.K., and F. Klein; methodology, H.G., K.V., L.E.S., F. Kurth, C.K., and F. Klein; investigation, H.G. and K.V.; resources, P.T-L., M.K., M.Z., F.M., H.J., M.A., and P.S.; formal analysis, H.G., K.V., and C.K.; writing-original draft, H.G., K.V., C.K., and F. Klein; writing-review and editing, M.K., P.T-L., and F. Kurth; visualization, H.G., K.V., C.K., and F. Klein; supervision, L.E.S., F. Kurth, and F. Klein; funding acquisition, L.E.S., F. Kurth, and F. Klein.

Declaration of interests

H.G., K.V., M.Z., C.K., and F. Klein are listed as inventors on patent applications on SARS-CoV-2-neutralizing antibodies encompassing aspects of this work filed by the University of Cologne.

Figure legends

Figure 1. Omicron sublineage differences.

(A) Spike amino acid changes in the BA.1, BA.1.1, and BA.2 Omicron sublineages relative to Wu01. **(B)** Locations of changed amino acids in Omicron sublineages highlighted on the SARS-CoV-2 spike (PDB: 6XR8). Representations on the right show RBD and NTD outlined in black. Changes exclusive to BA.2 are indicated in dark red (visible on surface) and light red (not visible). In **(A)** and **(B),** mutations shared between BA.1 and BA.1.1 are shown in orange, mutations shared between BA.1, BA.1.1 and BA.2 are shown in blue, the R346K mutation exclusive to BA.1.1 is shown in green, and mutations exclusive to BA.2 are shown in red. **(C)** Proportion of sequences submitted to the GISAID SARS-CoV-2 database per variant and week (accessed on April 2, 2022). NTD, N-terminal domain; RBD, receptor-binding domain; PDB, Protein Data Bank.

Figure 2. Omicron sublineage-neutralizing serum activity in vaccinated and convalescent individuals.

(A) Study scheme in COVID-19-convalescent individuals. Samples were collected after infection occurring between February and April, 2020 (V1), and after a BNT162b2 booster immunization (V2). **(B)** Fifty-percent inhibitory serum dilutions (ID_{50}s) against Wu01, BA.1, BA.1.1, and BA.2 determined by pseudovirus neutralization assays in

convalescent individuals. Bars indicate geometric mean ID_{50}s with 95% confidence intervals (CIs) at V1 (left) and V2 (right). Numbers indicate geometric mean ID_{50}s and percentage of individuals with detectable neutralizing activity (ID_{50} >10) in parentheses. **(C)** Correlation plots of log_{10} serum ID_{50}s against Wu01 (top) and BA.1 (bottom) versus BA.2 at V2 in convalescent individuals. r_s indicates Spearman's rank correlation coefficients. **(D)** Study scheme in vaccinated individuals. Samples were collected after the second dose of BNT162b2 (V1) and after the third dose of BNT162b2 (V2). **(E)** Serum ID_{50}s against Wu01, BA.1, BA.1.1, and BA.2 determined by pseudovirus neutralization assays in vaccinated individuals. Bars indicate geometric mean ID_{50}s with 95% CIs at V1 (left) and V2 (right). Numbers indicate geometric mean ID_{50}s and percentage of individuals with detectable neutralizing activity (ID_{50} >10) in parentheses. **(F)** Correlation plots of log_{10} serum ID_{50}s against Wu01 (top) and BA.1 (bottom) versus BA.2 at V2 in vaccinated individuals. r_s indicates Spearman's rank correlation coefficients. In **(B)** and **(E)**, ID_{50}s below the lower limit of quantification (LLOQ, ID_{50} of 10; indicated by black dotted lines) were imputed to ½ LLOQ (ID_{50}=5). In **(B)** and **(C)**, ID_{50}s above the upper limit of quantification (21,870) were imputed to 21,871.

Figure 3. Determining Omicron sublineage immune escape using monoclonal antibodies.

(A) SARS-CoV-2-neutralizing monoclonal antibodies (*n*=158) derived from 19 studies and isolated from ≥43 convalescent individuals were analyzed. Bar charts indicate number of antibodies per heavy chain variable gene segment (V_H), amino acid (aa) length of the heavy chain complementarity-determining region 3 (CDRH3), and number of V_H aa mutations relative to the V_H germline gene. Pie chart indicates antibody epitopes with slice sizes proportional to the number of antibodies. **(B)** Fraction of monoclonal

antibodies neutralizing (IC_{50} <10 µg/ml) Wu01 (green), BA.1 (light red), BA.1.1 (dark red), and BA.2 (blue) in pseudovirus neutralization assay. **(C)** IC_{50}s of antibodies with neutralizing activity (IC_{50} <10 µg/ml) against the individual variants (Wu01, *n*=158; BA.1, *n*=29; BA.1.1, *n=27*; BA.2, *n=34*). Bars depict geometric mean IC_{50}s and dotted line indicates lower limit of quantification (LLOQ, 0.005 µg/ml). **(D)** Spider plot of IC_{50}s for all antibodies against Wu01, BA.1, BA.1.1, and BA.2. Antibodies are sorted arbitrarily but equally for each virus. **(E)** Correlation plots of IC_{50}s of all antibodies against BA.1.1 (left) and BA.2 (right) versus BA.1. Colors indicate epitopes as in (**A**). Dashed lines represent identity lines and dotted lines indicate limits of quantification. **(F)** Bar charts of antibodies with neutralizing activity (IC_{50} <10 µg/ml) against any Omicron sublineage (*n*=40). Antibodies in each chart are sorted by BA.1-neutralizing activity (black outline) and bars show IC_{50}s against indicated sublineages. Dotted lines show LLOQ (0.005 µg/ml) and upper limit of quantification (ULOQ; 10 µg/ml). **(G)** Ratio (log_{10}) of IC_{50}s against BA.1 and BA.2 for all neutralizing antibodies with any Omicron sublineage-neutralizing activity (IC_{50} <10 µg/ml; *n*=40). Ratios >1 log_{10} are highlighted in green and percentage of antibodies with ratio >1 log_{10} is indicated. In **(E)-(G)**, IC_{50} <LLOQ were imputed to ½ LLOQ (IC_{50}=0.0025) and IC_{50} values >ULOQ were imputed to 2x ULOQ (IC_{50}=20). **(H)** Phylogenetic tree and sequence alignment of antibodies of the V_H3-53/3-66|V_K1-9 public clonotype. Letters indicate aa mutations relative to the V_H germline gene. Number of aa mutations compared to the corresponding germline allele and neutralizing activity against Wu01, BA.1, BA.1.1, and BA.2 are indicated on the right. Germline V_H represents the consensus of all identified germline alleles of depicted antibodies (V_H3-53*01, V_H3-53*04, and V_H3-66*01).

Figure 4. Omicron sublineage-neutralizing activity of monoclonal antibodies in clinical use.

(A) Dose response curves showing % neutralization of monoclonal antibodies against Wu01, BA.1, BA.1.1, and BA.2 in pseudovirus neutralization assay. Circles show averages and error bars indicate standard deviation. Dotted lines indicate 50% neutralization (IC_{50}). **(B)** IC_{50}s against Wu01, BA.1, BA.1.1, and BA.2 of monoclonal antibodies with current or previous authorization for clinical use or in clinical development. Symbols indicate whether clinical products or parental antibodies produced as human IgG1 were used.

Supplementary figure legends

Figure S1. Serum neutralization of Omicron sublineages.

(A) Serum ID_{50}s against Wu01, BA.1, BA.1.1, and BA.2 in the cohort of convalescent individuals after infection (V1) and BNT162b2 booster immunization (V2) as in **Figure 2**. Lines connect ID_{50}s of individual participants at V1 and V2. **(B)** Correlation plots of $\log_{10}$ serum ID_{50}s against indicated viruses in convalescent individuals at V2. r_s indicates Spearman's rank correlation coefficients. **(C)** Serum ID_{50}s against Wu01, BA.1, BA.1.1, and BA.2 in the cohort of BNT162b2-vaccinated individuals after the second (V1) and the third vaccine dose (V2) as in **Figure 2**. Lines connect ID_{50}s of individual participants at V1 and V2. **(D)** Correlation plots of $\log_{10}$ serum ID_{50}s against indicated viruses in vaccinated individuals at V2. r_s indicates Spearman's rank correlation coefficients.

Figure S2. Sequence mutations in Omicron-neutralizing antibodies.

Number of antibody V_H amino acid mutations compared to V_H germline sequence for antibodies not neutralizing (IC_{50} >10 µg/ml) any of the Omicron sublineages (left) or neutralizing at least one of the Omicron sublinages (right). Lines indicate mean and error bars indicate standard deviation. Statistical significance was determined using a two-sided Mann-Whitney U test.

Figure S3. Omicron sublineage-neutralizing activity of monoclonal antibodies in clinical testing.

Dose response curves showing % neutralization of monoclonal antibodies against Wu01, BA.1, BA.1.1, and BA.2 in a pseudovirus neutralization assay. Circles show averages and error bars indicate standard deviation. Dotted lines indicate 50% neutralization (IC_{50}).

Supplementary tables

Table S1: Study cohorts

Table S2: Monoclonal antibody panel analyses

Methods

Study cohort and sample collection

Serum samples from COVID-19-convalescent individuals were collected at the University Hospital Cologne under study protocols approved by the ethics committee (EC) of the Medical Faculty of the University of Cologne (16-054 and 20-1187). Between April and May, 2020, individuals with a history of SARS-CoV-2 infection confirmed by polymerase

chain reaction (documented through a written test certificate or as reported to study investigators by the participants) were enrolled within eight weeks of symptom onset and/or diagnosis. As all participants were enrolled early during the pandemic (i.e., prior to the emergence of variants of concern, as designated by the World Health Organization), most individuals are likely to have been infected with an early viral strain similar to Wu01. Participants were followed longitudinally to analyze long-term immunity to SARS-CoV-2.

Serum samples from vaccinated individuals were collected under protocols approved by the EC of Charité - Universitätsmedizin Berlin (EICOV, EA4/245/20) as well as the EC of the Federal State of Berlin and the Paul Ehrlich Institute (COVIM, EudraCT-No. 2021-001512-28). Study participation irrespective of medical conditions was offered to health-care workers vaccinated at the Charité – Universitätsmedizin (Berlin, Germany). All serum samples were tested for antibodies targeting the SARS-CoV-2 nucleocapsid using the SeraSpot Anti-SARS-CoV-2 IgG microarray-based immunoassay (Seramun Diagnostica). Samples from individuals with a history of SARS-CoV-2 infection, a positive SARS-CoV-2 nucleic acid amplification test (performed at sampling), or detectable anti-nucleocapsid antibodies were not included in this analysis.

All study participants provided written informed consent. Vaccinations in both cohorts were performed as part of routine care outside of the observational studies. Selection of participants and samples for analysis was based on receipt of identical vaccines and comparable sampling time points relative to vaccinations. Serum samples were collected after centrifugation and stored at -80°C until analysis.

SARS-CoV-2 pseudovirus constructs

All SARS-CoV-2 spike proteins were expressed using codon-optimized expression plasmids. Wu01 (EPI_ISL_406716) pseudoviruses were produced using an expression

plasmid that incorporated a C-terminal deletion of 21 cytoplasmic amino acids that result in increased pseudovirus titers. Expression plasmids for Omicron sublinage spike proteins were produced by assembling and cloning codon-optimized overlapping gene fragments (Thermo Fisher) into the pCDNA3.1/V5-HisTOPO vector (Thermo Fisher) using the NEBuilder HiFi DNA Assembly Kit (New England Biolabs), and included the full spike protein amino acid sequences with the following amino acid changes relative to Wu01:

BA.1: A67V, Δ69-70, T95I, G142D, Δ143-145, N211I, Δ212, ins215EPE, G339D, S371L, S373P, S375F, K417N, N440K, G446S, S477N, T478K, E484A, Q493R, G496S, Q498R, N501Y, Y505H, T547K, D614G, H655Y, N679K, P681H, N764K, D796Y, N856K, Q954H, N969K, and L981F.

BA.1.1: As for BA.1 with an additional R346K mutation.

BA.2: T19I, Δ24-26, A27S, A67V, G142D, V213G, G339D, S371F, S373P, S375F, T376A, D405N, R408S, K417N, N440K, S477N, T478K, E484A, Q493R, Q498R, N501Y, Y505H, D614G, H655Y, N679K, P681H, N764K, D796Y, Q954H, N969K.

All plasmid sequences were verified by sequencing.

Monoclonal antibodies

Monoclonal antibodies previously isolated in our lab had been obtained by single cell-sorting of SARS-CoV-2 spike-specific B cells followed by reverse transcription, PCR amplification and cloning of antibody variable regions (Kreer et al., 2020; Vanshylla et al., 2022). For monoclonal antibodies derived from the CoV-AbDab (Raybould et al., 2021), variable region amino acid sequences were reverse translated with the reverse translate tool from the Sequence Manipulation Suite (Stothard, 2000) using the *Homo sapiens* codon table obtained from the Codon Usage Database (Nakamura et al., 2000), and

460 sequences were ordered as gene fragments from Integrated DNA Technologies (IDT) with
461 5' and 3' overhangs. The variable regions were inserted into heavy and light chain
462 expression plasmids (Tiller et al., 2008) by sequence- and ligation-independent cloning
463 (SLIC). For antibodies ADG-2, COV2-2130, COV2-2196, COV2-2381, MAD0004J08, and
464 P2C-1F11, gene fragments based on the nucleotide sequences published in GenBank were
465 ordered at IDT and cloned as above. For antibodies C135, CT-P59, and LY-CoV1404, gene
466 fragments based on antibody structures deposited in the Protein Data Bank (accession
467 nos. 7K8Z, 7CM4, and 7MMO) were ordered at IDT after codon optimization using the IDT
468 Codon Optimization Tool and cloned as above. For antibodies 47D11, BD-368-2, C144,
469 and P2B-2F6, amino acid sequences were derived from CoV-AbDaB, corresponding
470 nucleotide sequences generated and codon-optimized using the IDT Codon Optimization
471 Tool, and gene fragments cloned as above.

472 Monoclonal antibody production was performed using 293-6E cells (National
473 Research Council of Canada) by co-transfection of heavy and light chain expression
474 plasmids using 25 kDa branched polyethylenimine (Sigma-Aldrich). Culture supernatants
475 were harvested after an incubation period of 6-7 days at 37°C and 6% CO2 under constant
476 shaking in FreeStyle Expression Medium supplemented with penicillin (20 U/ml) and
477 streptomycin (20 µg/ml) (all Thermo Fisher). Clarified cell supernatants were incubated
478 with Protein G Sepharose 4 FastFlow (Cytiva) overnight at 4°C . After centrifugation,
479 antibodies bound to Protein G beads were eluted in chromatography columns (Bio-Rad)
480 using 0.1 M glycine (pH=3.0) and buffered in 1 M Tris (pH=8.0). Buffer exchange to PBS
481 was performed using centrifugal filter units (Millipore). For antibodies bamlanivimab,
482 casirivimab, DZIF-10c, etesevimab, imdevimab, and sotrovimab, aliquots from clinical
483 stocks were used.
484

Pseudovirus neutralization assays

Neutralization assays were performed using lentivirus-based pseudoviruses and ACE2-expressing 293T cells (Crawford et al., 2020; Vanshylla et al., 2021). Pseudovirus particle production was performed in HEK293T cells by co-transfection of individual expression plasmids encoding for the SARS-CoV-2 spike protein, HIV-1 Tat, HIV-1 Gag/Pol, HIV-1 Rev, and luciferase-IRES-ZsGreen using FuGENE 6 Transfection Reagent (Promega). Culture supernatants were exchanged with fresh medium (high glucose DMEM supplemented with 2 mM L-glutamine, 100 IU/ml penicillin, 100 µg/ml streptomycin, 1 mM sodium pyruvate (all Thermo Fisher), and 10% FBS (Sigma-Aldrich)) 24 h post transfection. Pseudovirus-containing supernatants were harvested between 48-72 h after transfection, centrifuged, clarified using a 0.45 µm filter, and stored at -80°C. Pseudoviruses were titrated by infection of 293T-ACE2 cells and luciferase activity was determined after a 48-hour incubation at 37°C and 5% CO_2 by addition of luciferin/lysis buffer (10 mM $MgCl_2$, 0.3 mM ATP, 0.5 mM coenzyme A, 17 mM IGEPAL CA-630 (all Sigma-Aldrich), and 1 mM D-Luciferin (GoldBio) in Tris-HCL) using a microplate reader (Berthold).

Serum samples were heat-inactivated at 56°C for 45 min before use. Three-fold serial dilutions of serum (starting at 1:10) and monoclonal antibodies (starting at 10 µg/ml) were prepared in culture medium and co-incubated with pseudovirus supernatants for one hour at 37°C and 5% CO_2 prior to addition of 293T-ACE2 cells. Following a 48-hour incubation at 37°C and 5% CO_2, luciferase activity was determined as described above. Average background relative light units (RLUs) of non-infected cells were subtracted, and serum ID_{50}s and antibody IC_{50}s were determined as the serum dilutions and antibody concentrations resulting in a 50% RLU reduction compared to the average of virus-infected untreated controls cells using a non-linear fit model plotting an agonist vs. normalized dose response curve with variable slope using the least squares

fitting method in Prism 7.0 (GraphPad). All serum and monoclonal antibody samples were tested in duplicates. Imputation rules for values outside the limits of quantification are described below (see Statistical methods).

SARS-CoV-2 neutralizing antibody panel and sequence analysis

The panel of 158 SARS-CoV-2-neutralizing monoclonal antibodies isolated from SARS-CoV-2 convalescent individuals included in the analysis in **Figure 3** is based on 79 antibodies obtained in our previous work (Kreer et al., 2020; Vanshylla et al., 2022), 67 randomly selected (retrieved on January 1, 2021) human SARS-CoV-2-neutralizing antibodies deposited at CoV-AbDab (Raybould et al., 2021), and 12 antibodies in clinical use or development. We did not include five of the antibodies in clinical development shown in **Figure 4** into this analysis, as they were obtained from individuals infected with SARS-CoV (ADG-2, sotrovimab), from immunized mice harboring human immunglobulin gene repertoires (47D11, casirivimab), or using phage display technology that does not ensure native pairing of antibody heavy and light chains (CT-P59). For antibody DZIF-10c, the parental antibody (HbnC3t1p1_F4) was included in the analysis in **Figure 3**, while the clinical product is included in **Figure 4**.

Antibody amino acid sequences were annotated with IgBLASTp (Ye et al., 2013) based on the IMGT database (Lefranc, 2011). For sequence statistics, top V gene calls were counted without individual alleles, CDR3 lengths are reported according to the IMGT numbering system and numbers of V_H mutations refer to the top V gene call from IgBLASTp. Phylogenetic analysis of antibodies belonging to the V_H3-53/3-66|V_K1-9 public clonotype was performed by alignment of amino acid sequences with the MAFFT algorithm (Katoh et al., 2002) via the EMBL-EBI search and sequence analysis tools API (Madeira et al., 2019) and the Tree Builder tool from Geneious Prime 2020.0.4

(Biomatters) using the Jukes-Cantor distance model for tree building with the neighbour-joining method without resampling. Data aggregation and visualization was performed with the Python libraries pandas (v1.1.5), NumPy (v1.19.2), SciPy (v1.5.2), Matplotlib (v3.3.4) with Python (v3.6.8), as well as Microsoft Excel 2011 for Mac (v14.7.3), and Adobe Illustrator.

Visualization of SARS-CoV-2 spike amino acid changes

Amino acid changes relative to the Wu01 spike protein were visualized on a cryo-electron microscopy 3D-reconstruction of the SARS-CoV-2 spike protein (PDB ID: 6XR8) (Cai et al., 2020) using ChimeraX (v. 1.3) (Goddard et al., 2018; Pettersen et al., 2021).

SARS-CoV-2 variant distribution

GISAID-curated clade and lineage statistics of sequences submitted to the GISIAD database (Elbe and Buckland-Merrett, 2017; Khare et al., 2021; Shu and McCauley, 2017) were retrieved from GISAID (accessed on April 2, 2022) and frequency of individual variants was plotted as fraction of all submitted sequences per week and variant.

Statistical Methods

For graphical representation and statistical evaluation of serum samples in **Figures 2** and **S1**, samples that did not achieve 50% inhibition at the lowest tested dilution of 10 (lower limit of quantification, LLOQ) were imputed to ½ of the LLOQ (ID_{50}=5) and serum samples with ID_{50} >21,870 (upper limit of quantification) were imputed to ID_{50}=21871. For graphical representation and statistical analysis of monoclonal neutralizing antibodies in **Figure 3**, IC_{50} values of antibodies with an IC_{50} <0.005 µg/ml (LLOQ) were imputed to ½ LLOQ (IC_{50}=0.0025) and IC_{50} values >10 µg/ml (ULOQ) were imputed to 2x ULOQ (IC_{50}=20

µg/ml). Spearman's rank correlation coefficients were determined using Prism 7.0 (GraphPad; serum samples) or the spearmanr() function of the SciPy-package (v 1.5.2) stats-module (monoclonal antibodies). For the comparison of the number of V_H amino acid mutations relative to germline between antibodies neutralizing Wu01 or any Omicron sublineage, a two-sided Mann-Whitney U test was performed using the mannwhitneyu() function of the SciPy-package (v 1.5.2) stats-module.

Data and code availability

Requests for data or materials should be directed to the corresponding author and may be subject to restrictions based on data and privacy protection regulations and/or may require a Material Transfer Agreement (MTA). The paper does not report original code.

References

Altarawneh, H.N., Chemaitelly, H., Hasan, M.R., Ayoub, H.H., Qassim, S., AlMukdad, S., Coyle, P., Yassine, H.M., Al-Khatib, H.A., Benslimane, F.M., et al. (2022). Protection against the Omicron Variant from Previous SARS-CoV-2 Infection. N Engl J Med.

Andrews, N., Stowe, J., Kirsebom, F., Toffa, S., Rickeard, T., Gallagher, E., Gower, C., Kall, M., Groves, N., O'Connell, A.-M., et al. (2022). Covid-19 Vaccine Effectiveness against the Omicron (B.1.1.529) Variant. New England Journal of Medicine.

Barnes, C.O., West, A.P., Jr., Huey-Tubman, K.E., Hoffmann, M.A.G., Sharaf, N.G., Hoffman, P.R., Koranda, N., Gristick, H.B., Gaebler, C., Muecksch, F., et al. (2020). Structures of Human Antibodies Bound to SARS-CoV-2 Spike Reveal Common Epitopes and Recurrent Features of Antibodies. Cell 182, 828-842 e816.

Cai, Y., Zhang, J., Xiao, T., Peng, H., Sterling, S.M., Walsh, R.M., Jr., Rawson, S., Rits-Volloch, S., and Chen, B. (2020). Distinct conformational states of SARS-CoV-2 spike protein. Science 369, 1586-1592.

Cao, Y., Su, B., Guo, X., Sun, W., Deng, Y., Bao, L., Zhu, Q., Zhang, X., Zheng, Y., Geng, C., et al. (2020). Potent Neutralizing Antibodies against SARS-CoV-2 Identified by High-Throughput Single-Cell Sequencing of Convalescent Patients' B Cells. Cell 182, 73-84 e16.

Cao, Y., Wang, J., Jian, F., Xiao, T., Song, W., Yisimayi, A., Huang, W., Li, Q., Wang, P., An, R., et al. (2022). Omicron escapes the majority of existing SARS-CoV-2 neutralizing antibodies. Nature 602, 657-663.

592 Carreno, J.M., Alshammary, H., Tcheou, J., Singh, G., Raskin, A.J., Kawabata, H., Sominsky,
593 L.A., Clark, J.J., Adelsberg, D.C., Bielak, D.A., et al. (2022). Activity of convalescent and
594 vaccine serum against SARS-CoV-2 Omicron. Nature 602, 682-688.

595 Cele, S., Jackson, L., Khoury, D.S., Khan, K., Moyo-Gwete, T., Tegally, H., San, J.E., Cromer, D.,
596 Scheepers, C., Amoako, D.G., et al. (2022). Omicron extensively but incompletely escapes
597 Pfizer BNT162b2 neutralization. Nature 602, 654-656.

598 Cheng, S.M.S., Mok, C.K.P., Leung, Y.W.Y., Ng, S.S., Chan, K.C.K., Ko, F.W., Chen, C., Yiu, K.,
599 Lam, B.H.S., Lau, E.H.Y., et al. (2022). Neutralizing antibodies against the SARS-CoV-2
600 Omicron variant BA.1 following homologous and heterologous CoronaVac or BNT162b2
601 vaccination. Nat Med.

602 Cohen, M.S., Nirula, A., Mulligan, M.J., Novak, R.M., Marovich, M., Yen, C., Stemer, A., Mayer,
603 S.M., Wohl, D., Brengle, B., et al. (2021). Effect of Bamlanivimab vs Placebo on Incidence of
604 COVID-19 Among Residents and Staff of Skilled Nursing and Assisted Living Facilities: A
605 Randomized Clinical Trial. JAMA 326, 46-55.

606 Corti, D., Purcell, L.A., Snell, G., and Veesler, D. (2021). Tackling COVID-19 with
607 neutralizing monoclonal antibodies. Cell 184, 3086-3108.

608 Crawford, K.H.D., Eguia, R., Dingens, A.S., Loes, A.N., Malone, K.D., Wolf, C.R., Chu, H.Y.,
609 Tortorici, M.A., Veesler, D., Murphy, M., et al. (2020). Protocol and Reagents for
610 Pseudotyping Lentiviral Particles with SARS-CoV-2 Spike Protein for Neutralization
611 Assays. Viruses 12.

612 Dougan, M., Nirula, A., Azizad, M., Mocherla, B., Gottlieb, R.L., Chen, P., Hebert, C., Perry, R.,
613 Boscia, J., Heller, B., et al. (2021). Bamlanivimab plus Etesevimab in Mild or Moderate
614 Covid-19. N Engl J Med 385, 1382-1392.

615 Elbe, S., and Buckland-Merrett, G. (2017). Data, disease and diplomacy: GISAID's
616 innovative contribution to global health. Glob Chall 1, 33-46.

617 Feng, S., Phillips, D.J., White, T., Sayal, H., Aley, P.K., Bibi, S., Dold, C., Fuskova, M., Gilbert,
618 S.C., Hirsch, I., et al. (2021). Correlates of protection against symptomatic and
619 asymptomatic SARS-CoV-2 infection. Nat Med 27, 2032-2040.

620 Garcia-Beltran, W.F., St Denis, K.J., Hoelzemer, A., Lam, E.C., Nitido, A.D., Sheehan, M.L.,
621 Berrios, C., Ofoman, O., Chang, C.C., Hauser, B.M., et al. (2022). mRNA-based COVID-19
622 vaccine boosters induce neutralizing immunity against SARS-CoV-2 Omicron variant. Cell
623 185, 457-466 e454.

624 Goddard, T.D., Huang, C.C., Meng, E.C., Pettersen, E.F., Couch, G.S., Morris, J.H., and Ferrin,
625 T.E. (2018). UCSF ChimeraX: Meeting modern challenges in visualization and analysis.
626 Protein Sci 27, 14-25.

627 Greaney, A.J., Starr, T.N., Barnes, C.O., Weisblum, Y., Schmidt, F., Caskey, M., Gaebler, C.,
628 Cho, A., Agudelo, M., Finkin, S., et al. (2021). Mapping mutations to the SARS-CoV-2 RBD
629 that escape binding by different classes of antibodies. Nat Commun 12, 4196.

Group, R.C. (2022). Casirivimab and imdevimab in patients admitted to hospital with COVID-19 (RECOVERY): a randomised, controlled, open-label, platform trial. The Lancet 399, 665-676.

Gruell, H., Vanshylla, K., Tober-Lau, P., Hillus, D., Schommers, P., Lehmann, C., Kurth, F., Sander, L.E., and Klein, F. (2022). mRNA booster immunization elicits potent neutralizing serum activity against the SARS-CoV-2 Omicron variant. Nat Med.

Gupta, A., Gonzalez-Rojas, Y., Juarez, E., Crespo Casal, M., Moya, J., Falci, D.R., Sarkis, E., Solis, J., Zheng, H., Scott, N., et al. (2021). Early Treatment for Covid-19 with SARS-CoV-2 Neutralizing Antibody Sotrovimab. N Engl J Med 385, 1941-1950.

Harvey, W.T., Carabelli, A.M., Jackson, B., Gupta, R.K., Thomson, E.C., Harrison, E.M., Ludden, C., Reeve, R., Rambaut, A., Consortium, C.-G.U., et al. (2021). SARS-CoV-2 variants, spike mutations and immune escape. Nat Rev Microbiol 19, 409-424.

Hillus, D., Schwarz, T., Tober-Lau, P., Vanshylla, K., Hastor, H., Thibeault, C., Jentzsch, S., Helbig, E.T., Lippert, L.J., Tscheak, P., et al. (2021). Safety, reactogenicity, and immunogenicity of homologous and heterologous prime-boost immunisation with ChAdOx1 nCoV-19 and BNT162b2: a prospective cohort study. The Lancet Respiratory Medicine 9, 1255-1265.

Hoffmann, M., Kruger, N., Schulz, S., Cossmann, A., Rocha, C., Kempf, A., Nehlmeier, I., Graichen, L., Moldenhauer, A.S., Winkler, M.S., et al. (2022). The Omicron variant is highly resistant against antibody-mediated neutralization: Implications for control of the COVID-19 pandemic. Cell 185, 447-456 e411.

Iketani, S., Liu, L., Guo, Y., Liu, L., Chan, J.F.W., Huang, Y., Wang, M., Luo, Y., Yu, J., Chu, H., et al. (2022). Antibody evasion properties of SARS-CoV-2 Omicron sublineages. Nature.

Katoh, K., Misawa, K., Kuma, K., and Miyata, T. (2002). MAFFT: a novel method for rapid multiple sequence alignment based on fast Fourier transform. Nucleic Acids Res 30, 3059-3066.

Khare, S., Gurry, C., Freitas, L., Schultz, M.B., Bach, G., Diallo, A., Akite, N., Ho, J., Lee, R.T., Yeo, W., et al. (2021). GISAID's Role in Pandemic Response. China CDC Wkly 3, 1049-1051.

Khoury, D.S., Cromer, D., Reynaldi, A., Schlub, T.E., Wheatley, A.K., Juno, J.A., Subbarao, K., Kent, S.J., Triccas, J.A., and Davenport, M.P. (2021). Neutralizing antibody levels are highly predictive of immune protection from symptomatic SARS-CoV-2 infection. Nat Med 27, 1205-1211.

Kreer, C., Zehner, M., Weber, T., Ercanoglu, M.S., Gieselmann, L., Rohde, C., Halwe, S., Korenkov, M., Schommers, P., Vanshylla, K., et al. (2020). Longitudinal Isolation of Potent Near-Germline SARS-CoV-2-Neutralizing Antibodies from COVID-19 Patients. Cell 182, 843-854 e812.

Kuhlmann, C., Mayer, C.K., Claassen, M., Maponga, T., Burgers, W.A., Keeton, R., Riou, C., Sutherland, A.D., Suliman, T., Shaw, M.L., et al. (2022). Breakthrough infections with SARS-CoV-2 omicron despite mRNA vaccine booster dose. The Lancet 399, 625-626.

669 Lefranc, M.P. (2011). IMGT, the International ImMunoGeneTics Information System. Cold
670 Spring Harb Protoc 2011, 595-603.

671 Liu, C., Ginn, H.M., Dejnirattisai, W., Supasa, P., Wang, B., Tuekprakhon, A., Nutalai, R., Zhou,
672 D., Mentzer, A.J., Zhao, Y., et al. (2021). Reduced neutralization of SARS-CoV-2 B.1.617 by
673 vaccine and convalescent serum. Cell 184, 4220-4236 e4213.

674 Liu, L., Iketani, S., Guo, Y., Chan, J.F., Wang, M., Liu, L., Luo, Y., Chu, H., Huang, Y., Nair, M.S.,
675 et al. (2022). Striking antibody evasion manifested by the Omicron variant of SARS-CoV-
676 2. Nature 602, 676-681.

677 Lyngse, F.P., Kirkeby, C.T., Denwood, M., Christiansen, L.E., Mølbak, K., Møller, C.H., Skov,
678 R.L., Krause, T.G., Rasmussen, M., Sieber, R.N., et al. (2022). Transmission of SARS-CoV-2
679 Omicron VOC subvariants BA.1 and BA.2: Evidence from Danish Households. medRxiv.

680 Madeira, F., Park, Y.M., Lee, J., Buso, N., Gur, T., Madhusoodanan, N., Basutkar, P., Tivey,
681 A.R.N., Potter, S.C., Finn, R.D., et al. (2019). The EMBL-EBI search and sequence analysis
682 tools APIs in 2019. Nucleic Acids Res 47, W636-W641.

683 Madhi, S.A., Kwatra, G., Myers, J.E., Jassat, W., Dhar, N., Mukendi, C.K., Nana, A.J., Blumberg,
684 L., Welch, R., Ngorima-Mabhena, N., et al. (2022). Population Immunity and Covid-19
685 Severity with Omicron Variant in South Africa. N Engl J Med.

686 Meng, B., Abdullahi, A., Ferreira, I., Goonawardane, N., Saito, A., Kimura, I., Yamasoba, D.,
687 Gerber, P.P., Fatihi, S., Rathore, S., et al. (2022). Altered TMPRSS2 usage by SARS-CoV-2
688 Omicron impacts tropism and fusogenicity. Nature.

689 Nakamura, Y., Gojobori, T., and Ikemura, T. (2000). Codon usage tabulated from
690 international DNA sequence databases: status for the year 2000. Nucleic Acids Res 28,
691 292.

692 Nielsen, S.C.A., Yang, F., Jackson, K.J.L., Hoh, R.A., Roltgen, K., Jean, G.H., Stevens, B.A., Lee,
693 J.Y., Rustagi, A., Rogers, A.J., et al. (2020). Human B Cell Clonal Expansion and Convergent
694 Antibody Responses to SARS-CoV-2. Cell Host Microbe 28, 516-525 e515.

695 O'Brien, M.P., Forleo-Neto, E., Musser, B.J., Isa, F., Chan, K.C., Sarkar, N., Bar, K.J., Barnabas,
696 R.V., Barouch, D.H., Cohen, M.S., et al. (2021). Subcutaneous REGEN-COV Antibody
697 Combination to Prevent Covid-19. N Engl J Med 385, 1184-1195.

698 Perez-Then, E., Lucas, C., Monteiro, V.S., Miric, M., Brache, V., Cochon, L., Vogels, C.B.F.,
699 Malik, A.A., De la Cruz, E., Jorge, A., et al. (2022). Neutralizing antibodies against the SARS-
700 CoV-2 Delta and Omicron variants following heterologous CoronaVac plus BNT162b2
701 booster vaccination. Nat Med.

702 Pettersen, E.F., Goddard, T.D., Huang, C.C., Meng, E.C., Couch, G.S., Croll, T.I., Morris, J.H.,
703 and Ferrin, T.E. (2021). UCSF ChimeraX: Structure visualization for researchers,
704 educators, and developers. Protein Sci 30, 70-82.

705 Planas, D., Saunders, N., Maes, P., Guivel-Benhassine, F., Planchais, C., Buchrieser, J.,
706 Bolland, W.H., Porrot, F., Staropoli, I., Lemoine, F., et al. (2022). Considerable escape of
707 SARS-CoV-2 Omicron to antibody neutralization. Nature 602, 671-675.

Qassim, S.H., Chemaitelly, H., Ayoub, H., AlMukdad, S., Tang, P., Hasan, M.R., Yassine, H.M., Al-Khatib, H.A., Smatti, M.K., Abdul Rahim, H.F., et al. (2022). Effects of BA.1/BA.2 subvariant, vaccination, and prior infection on infectiousness of SARS-CoV-2 Omicron infections. medRxiv.

Raybould, M.I.J., Kovaltsuk, A., Marks, C., and Deane, C.M. (2021). CoV-AbDab: the coronavirus antibody database. Bioinformatics 37, 734-735.

Robbiani, D.F., Gaebler, C., Muecksch, F., Lorenzi, J.C.C., Wang, Z., Cho, A., Agudelo, M., Barnes, C.O., Gazumyan, A., Finkin, S., et al. (2020). Convergent antibody responses to SARS-CoV-2 in convalescent individuals. Nature 584, 437-442.

Schmidt, F., Muecksch, F., Weisblum, Y., Da Silva, J., Bednarski, E., Cho, A., Wang, Z., Gaebler, C., Caskey, M., Nussenzweig, M.C., et al. (2022). Plasma Neutralization of the SARS-CoV-2 Omicron Variant. N Engl J Med 386, 599-601.

Shu, Y., and McCauley, J. (2017). GISAID: Global initiative on sharing all influenza data - from vision to reality. Euro Surveill 22.

Shuai, H., Chan, J.F., Hu, B., Chai, Y., Yuen, T.T., Yin, F., Huang, X., Yoon, C., Hu, J.C., Liu, H., et al. (2022). Attenuated replication and pathogenicity of SARS-CoV-2 B.1.1.529 Omicron. Nature.

Stothard, P. (2000). The sequence manipulation suite: JavaScript programs for analyzing and formatting protein and DNA sequences. Biotechniques 28, 1102, 1104.

Tiller, T., Meffre, E., Yurasov, S., Tsuiji, M., Nussenzweig, M.C., and Wardemann, H. (2008). Efficient generation of monoclonal antibodies from single human B cells by single cell RT-PCR and expression vector cloning. J Immunol Methods 329, 112-124.

Tseng, H.F., Ackerson, B.K., Luo, Y., Sy, L.S., Talarico, C.A., Tian, Y., Bruxvoort, K.J., Tubert, J.E., Florea, A., Ku, J.H., et al. (2022). Effectiveness of mRNA-1273 against SARS-CoV-2 Omicron and Delta variants. Nat Med.

VanBlargan, L.A., Errico, J.M., Halfmann, P.J., Zost, S.J., Crowe, J.E., Jr., Purcell, L.A., Kawaoka, Y., Corti, D., Fremont, D.H., and Diamond, M.S. (2022). An infectious SARS-CoV-2 B.1.1.529 Omicron virus escapes neutralization by therapeutic monoclonal antibodies. Nat Med.

Vanshylla, K., Di Cristanziano, V., Kleipass, F., Dewald, F., Schommers, P., Gieselmann, L., Gruell, H., Schlotz, M., Ercanoglu, M.S., Stumpf, R., et al. (2021). Kinetics and correlates of the neutralizing antibody response to SARS-CoV-2 infection in humans. Cell Host Microbe 29, 917-929 e914.

Vanshylla, K., Fan, C., Wunsch, M., Poopalasingam, N., Meijers, M., Kreer, C., Kleipass, F., Ruchnewitz, D., Ercanoglu, M.S., Gruell, H., et al. (2022). Discovery of ultrapotent broadly neutralizing antibodies from SARS-CoV-2 elite neutralizers. Cell Host Microbe 30, 69-82 e10.

Viana, R., Moyo, S., Amoako, D.G., Tegally, H., Scheepers, C., Althaus, C.L., Anyaneji, U.J., Bester, P.A., Boni, M.F., Chand, M., et al. (2022). Rapid epidemic expansion of the SARS-CoV-2 Omicron variant in southern Africa. Nature.

747 Weinreich, D.M., Sivapalasingam, S., Norton, T., Ali, S., Gao, H., Bhore, R., Xiao, J., Hooper,
748 A.T., Hamilton, J.D., Musser, B.J., et al. (2021). REGEN-COV Antibody Combination and
749 Outcomes in Outpatients with Covid-19. N Engl J Med 385, e81.

750 Weissman, D., Alameh, M.G., de Silva, T., Collini, P., Hornsby, H., Brown, R., LaBranche, C.C.,
751 Edwards, R.J., Sutherland, L., Santra, S., et al. (2021). D614G Spike Mutation Increases
752 SARS CoV-2 Susceptibility to Neutralization. Cell Host Microbe 29, 23-31 e24.

753 Wratil, P.R., Stern, M., Priller, A., Willmann, A., Almanzar, G., Vogel, E., Feuerherd, M.,
754 Cheng, C.C., Yazici, S., Christa, C., et al. (2022). Three exposures to the spike protein of
755 SARS-CoV-2 by either infection or vaccination elicit superior neutralizing immunity to all
756 variants of concern. Nat Med.

757 Yamasoba, D., Kimura, I., Nasser, H., Morioka, Y., Nao, N., Ito, J., Uriu, K., Tsuda, M.,
758 Zahradnik, J., Shirakawa, K., et al. (2022). Virological characteristics of SARS-CoV-2 BA.2
759 variant. medRxiv.

760 Ye, J., Ma, N., Madden, T.L., and Ostell, J.M. (2013). IgBLAST: an immunoglobulin variable
761 domain sequence analysis tool. Nucleic Acids Res 41, W34-40.

762 Yuan, M., Liu, H., Wu, N.C., Lee, C.D., Zhu, X., Zhao, F., Huang, D., Yu, W., Hua, Y., Tien, H., et
763 al. (2020). Structural basis of a shared antibody response to SARS-CoV-2. Science 369,
764 1119-1123.

765 Zhang, Q., Ju, B., Ge, J., Chan, J.F., Cheng, L., Wang, R., Huang, W., Fang, M., Chen, P., Zhou, B.,
766 et al. (2021). Potent and protective IGHV3-53/3-66 public antibodies and their shared
767 escape mutant on the spike of SARS-CoV-2. Nat Commun 12, 4210.

768 Zhao, X., Li, D., Ruan, W., Chen, Z., Zhang, R., Zheng, A., Qiao, S., Zheng, X., Zhao, Y., Dai, L.,
769 et al. (2022). Effects of a Prolonged Booster Interval on Neutralization of Omicron Variant.
770 N Engl J Med 386, 894-896.

771

Figure 1

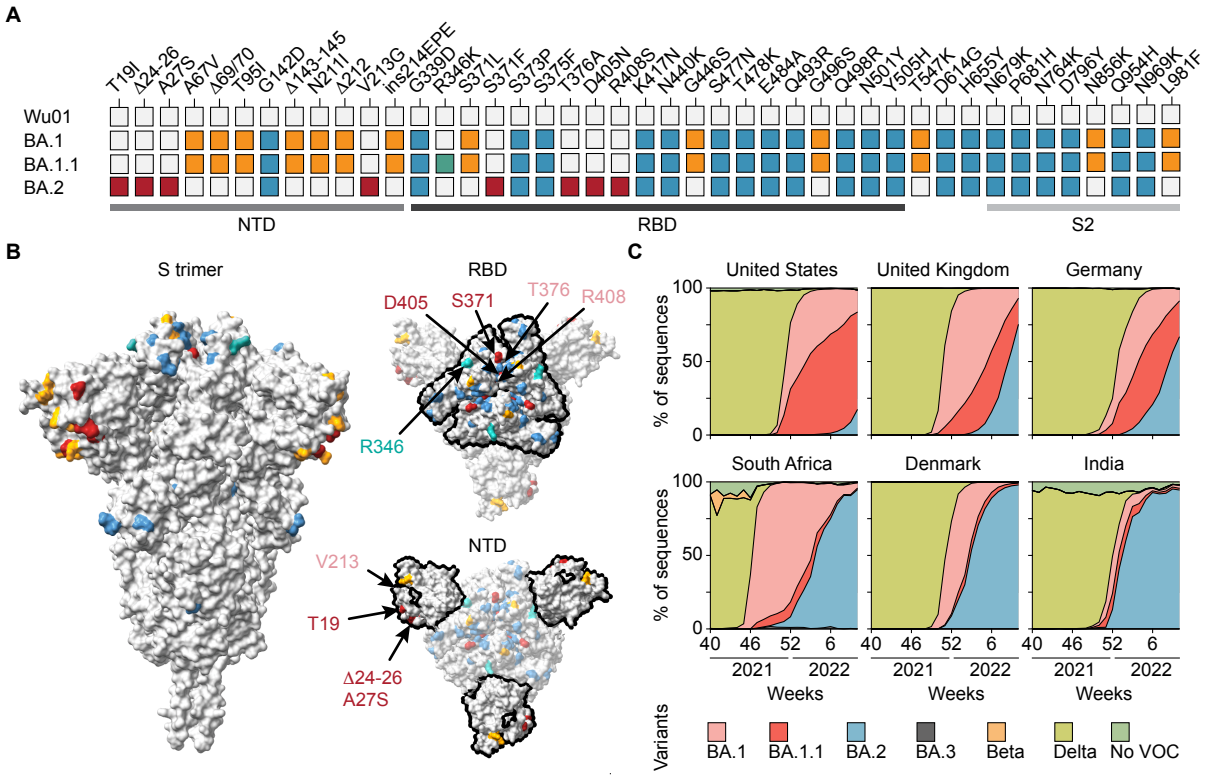

Figure 1. Omicron sublineage differences.
(A) Spike amino acid changes in the BA.1, BA.1.1, and BA.2 Omicron sublineages relative to Wu01. **(B)** Locations of changed amino acids in Omicron sublineages highlighted on the SARS-CoV-2 spike (PDB: 6XR8). Representations on the right show RBD and NTD outlined in black. Changes exclusive to BA.2 are indicated in dark red (visible on surface) and light red (not visible). In (A) and (B), mutations shared between BA.1 and BA.1.1 are shown in orange, mutations shared between BA.1, BA.1.1 and BA.2 are shown in blue, the R346K mutation exclusive to BA.1.1 is shown in green, and mutations exclusive to BA.2 are shown in red. **(C)** Proportion of sequences submitted to the GISAID SARS-CoV-2 database per variant and week (accessed on April 2, 2022). NTD, N-terminal domain; RBD, receptor-binding domain; PDB, Protein Data Bank.

Figure 2

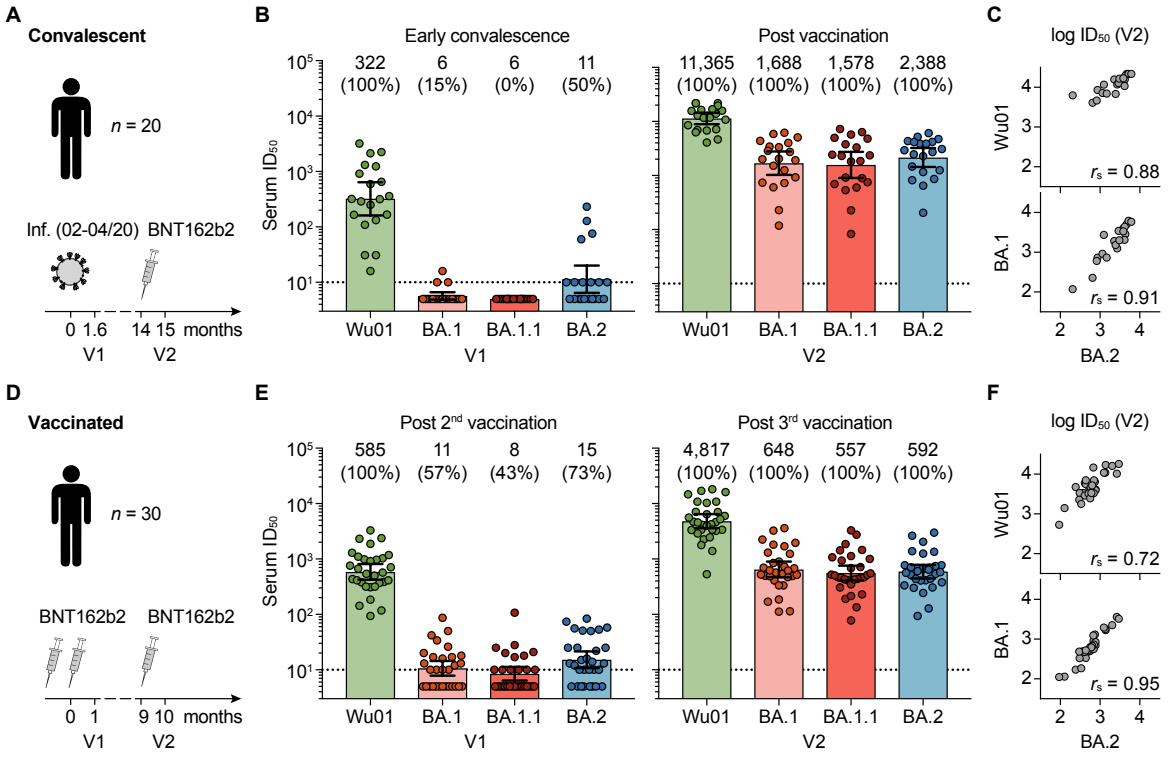

Figure 2. Omicron sublineage-neutralizing serum activity in vaccinated and convalescent individuals.
(A) Study scheme in COVID-19-convalescent individuals. Samples were collected after infection occurring between February and April, 2020 (V1), and after a BNT162b2 booster immunization (V2). **(B)** Fifty-percent inhibitory serum dilutions (ID_{50}s) against Wu01, BA.1, BA.1.1, and BA.2 determined by pseudovirus neutralization assays in convalescent individuals. Bars indicate geometric mean ID_{50}s with 95% confidence intervals (CIs) at V1 (left) and V2 (right). Numbers indicate geometric mean ID_{50}s and percentage of individuals with detectable neutralizing activity (ID_{50} >10) in parentheses. **(C)** Correlation plots of log_{10} serum ID_{50}s against Wu01 (top) and BA.1 (bottom) versus BA.2 at V2 in convalescent individuals. r_s indicates Spearman's rank correlation coefficients. **(D)** Study scheme in vaccinated individuals. Samples were collected after the second dose of BNT162b2 (V1) and after the third dose of BNT162b2 (V2). **(E)** Serum ID_{50}s against Wu01, BA.1, BA.1.1, and BA.2 determined by pseudovirus neutralization assays in vaccinated individuals. Bars indicate geometric mean ID_{50}s with 95% CIs at V1 (left) and V2 (right). Numbers indicate geometric mean ID_{50}s and percentage of individuals with detectable neutralizing activity (ID_{50} >10) in parentheses. **(F)** Correlation plots of log_{10} serum ID_{50}s against Wu01 (top) and BA.1 (bottom) versus BA.2 at V2 in vaccinated individuals. r_s indicates Spearman's rank correlation coefficients. In (B) and (E), ID_{50}s below the lower limit of quantification (LLOQ, ID_{50} of 10; indicated by black dotted lines) were imputed to ½ LLOQ (ID_{50}=5). In (B) and (C), ID_{50}s above the upper limit of quantification (21,870) were imputed to 21,871.

Figure 3

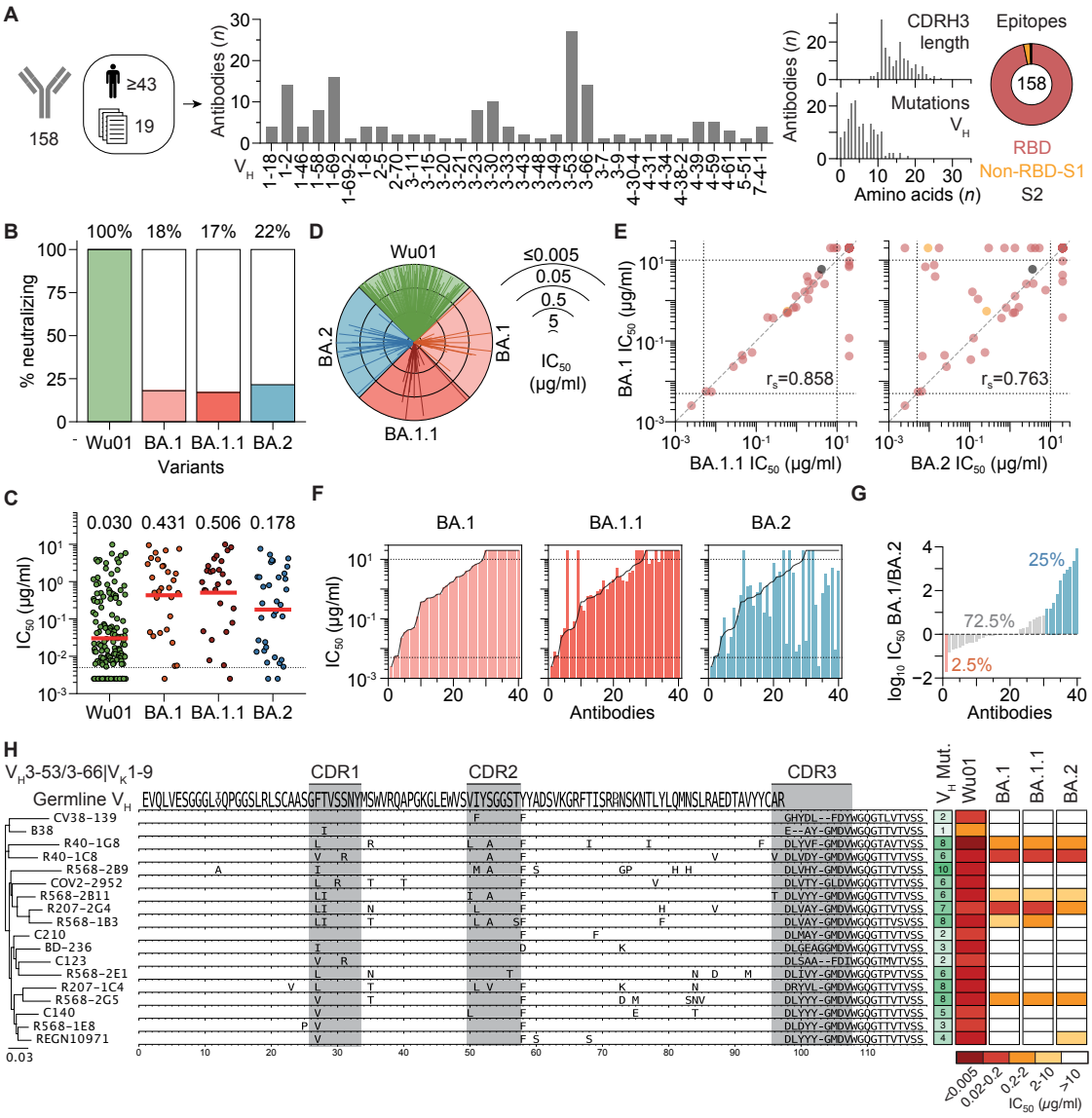

Figure 3. Determining Omicron sublineage immune escape using monoclonal antibodies.
(A) SARS-CoV-2-neutralizing monoclonal antibodies (n=158) derived from 19 studies and isolated from ≥43 convalescent individuals were analyzed. Bar charts indicate number of antibodies per heavy chain variable gene segment (V_H), amino acid (aa) length of the heavy chain complementarity-determining region 3 (CDRH3), and number of V_H aa mutations relative to the V_H germline gene. Pie chart indicates antibody epitopes with slice sizes proportional to the number of antibodies. **(B)** Fraction of monoclonal antibodies neutralizing (IC_{50} <10 μg/ml) Wu01 (green), BA.1 (light red), BA.1.1 (dark red), and BA.2 (blue) in pseudovirus neutralization assay. **(C)** IC_{50}s of antibodies with neutralizing activity (IC_{50} <10 μg/ml) against the individual variants (Wu01, n=158; BA.1, n=29; BA.1.1, n=27; BA.2, n=34). Bars depict geometric mean IC_{50}s and dotted line indicates lower limit of quantification (LLOQ, 0.005 μg/ml). **(D)** Spider plot of IC_{50}s for all antibodies against Wu01, BA.1, BA.1.1, and BA.2. Antibodies are sorted arbitrarily but equally for each virus. **(E)** Correlation plots of IC_{50}s of all antibodies against BA.1.1 (left) and BA.2 (right) versus BA.1. Colors indicate epitopes as in (A). Dashed lines represent identity lines and dotted lines indicate limits of quantification. **(F)** Bar charts of antibodies with neutralizing activity (IC_{50} <10 μg/ml) against any Omicron sublineage (n=40). Antibodies in each chart are sorted by BA.1-neutralizing activity (black outline) and bars show IC_{50}s against indicated sublineages. Dotted lines show LLOQ (0.005 μg/ml) and upper limit of quantification (ULOQ; 10 μg/ml). **(G)** Ratio (log_{10}) of IC_{50}s against BA.1 and BA.2 for all neutralizing antibodies with any Omicron sublineage-neutralizing activity (IC_{50} <10 μg/ml; n=40). Ratios >1 log_{10} are highlighted in green and percentage of antibodies with ratio >1 log_{10} is indicated. In (E)-(G), IC_{50} <LLOQ were imputed to ½ LLOQ (IC_{50}=0.0025) and IC_{50} values >ULOQ were imputed to 2x ULOQ (IC_{50}=20). **(H)** Phylogenetic tree and sequence alignment of antibodies of the V_H3-53/3-66|V_K1-9 public clonotype. Letters indicate aa mutations relative to the V_H germline gene. Number of aa mutations compared to the corresponding germline allele and neutralizing activity against Wu01, BA.1, BA.1.1, and BA.2 are indicated on the right. Germline V_H represents the consensus of all identified germline alleles of depicted antibodies (VH3-53*01, VH3-53*04, and VH3-66*01).

Figure 4

A

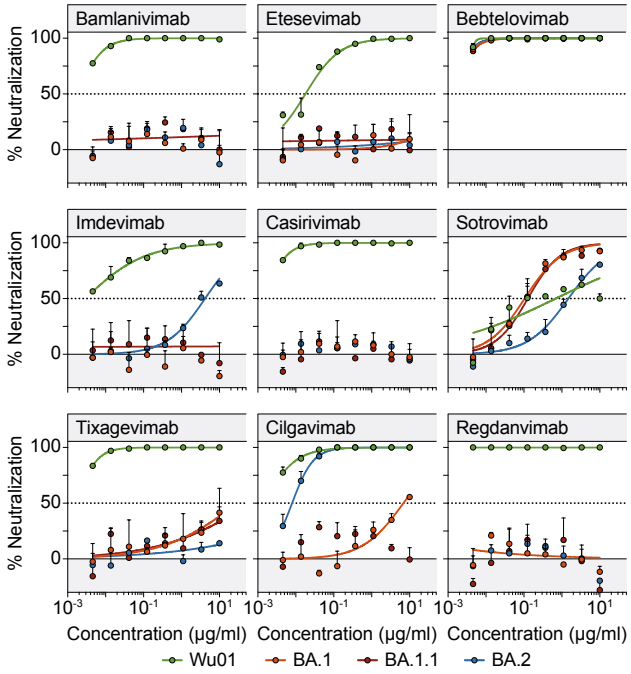

B

	Antibody		IC_{50} (μg/ml)			
	Clinical ID	Parental ID	Wu01	BA.1	BA.1.1	BA.2
Approved	Bamlanivimab*	LY-CoV555	<0.005	>10	>10	>10
	Etesevimab*	CB6/JS016	0.018	>10	>10	>10
	Bebtelovimab	LY-CoV1404†	<0.005	<0.005	<0.005	<0.005
	Imdevimab*	REGN10987	<0.005	>10	>10	4.173
	Casirivimab*	REGN10933	<0.005	>10	>10	>10
	Sotrovimab*	S309	0.685	0.105	0.127	1.488
	Tixagevimab	COV2-2196†	<0.005	>10	>10	>10
	Cilgavimab	COV2-2130†	<0.005	6.848	>10	0.008
	Regdanvimab	CT-P59†	<0.005	>10	>10	>10
In trials	DZIF-10c*	HbnC3t1p1_F4	<0.005	0.046	>10	0.033
	BRII-196	P2C-1F11†	<0.005	>10	>10	>10
	BMS-986414	C135†	<0.005	>10	>10	>10
	BMS-986413	C144†	<0.005	>10	>10	>10
	ADM03820§	COV2-2381†	0.008	>10	>10	>10
	ADG-20	ADG-2†	<0.005	0.212	0.194	>10
	ABBV-47D11	47D11†	0.386	>10	>10	>10
	BGB-DXP593	BD-368-2†	<0.005	>10	>10	>10
	n.a.	MAD0004J08†	<0.005	>10	>10	>10

* Clinical product used.
† Parental antibody (Fc-unmodified IgG1) used.
§ Combination product of COV2-2381 and COV2-2130.

Figure 4. Omicron sublineage-neutralizing activity of monoclonal antibodies in clinical use.
(A) Dose response curves showing % neutralization of monoclonal antibodies against Wu01, BA.1, BA.1.1, and BA.2 in pseudovirus neutralization assay. Circles show averages and error bars indicate standard deviation. Dotted lines indicate 50% neutralization (IC_{50}). **(B)** IC_{50}s against Wu01, BA.1, BA.1.1, and BA.2 of monoclonal antibodies with current or previous authorization for clinical use or in clinical development. Symbols indicate whether clinical products or parental antibodies produced as human IgG1 were used.